11

Development of the cryogenic load for 1.1−1.4 mm sideband separating SIS-mixer

© A.V. Khudchenko,[1,2] K.I. Rudakov,[1,2] I.V. Tretyakov,[1] A.M. Chekushkin,[2] I.A. Mutaev,[3] V.P. Koshelets[1,2]

[1]stro Space Center of P.N. Lebedev Physical Institute of the Russian Academy of Sciences,
117810 Moscow, Russia
[2]Kotelnikov Institute of Radio Engineering and Electronics, Russian Academy of Sciences,
125009 Moscow, Russia
[3]Moscow Institute of Physics and Technology (National Research University),
141701 Dolgoprudny, Moscow Region, Russia
e-mail: khudchenko@asc.rssi.ru

Received May 19, 2024
Revised May 19, 2024
Accepted May 19, 2024

This paper describes the design of a waveguide load for a cryogenic sideband separating receiver based on SIS mixers for the 1.1−1.4 mm range. The load is designed as a metal insert in the center of the waveguide. The insert is based on 125 μm thick quartz substrate with a deposited 8 nm thick NiCr film, which has a resistance of about 250 Ω/sq. Measurements demonstrate the variations of the film resistance to be within 5 percent while temperature changes from 300 to 4.2 K. Simulations show that the load reflection level can be expected to be less than −35 dB in the 220−330 GHz range.

Keywords: waveguide load, thin metal film, SIS waveguide mixers, sideband separating mixers.

DOI: 10.61011/TP.2024.08.58998.179-24

Introduction

The results of developing a cryogenic waveguide load presented in this paper constitute a part of a comprehensive effort for development of a highly sensitive receiver with sideband separation for the 211−275 GHz band (approximately 1.1−1.4 mm) based on superconductor-insulator-superconductor tunnel junctions (SIS). This receiver can be used for conducting unique astrophysical observations both as part of ground-based [1–6] telescopes, and on board space-based observatories such as Millimetron [7,8]. The need to place a receiver with sideband separation on board the Millimetron observatory is attributable to the fact that for the given range, all ground-based telescopes are equipped with this type of receiver, and not a more technically simple two-pole receiver. Therefore, it is necessary to have as similar receiving systems as possible in both arms for the most effective correlation of ground-based and space-based radio interferometer signals with an extremely long base. Only one band will correlate with the ground signal if a two-pole receiver is used on a space telescope, while the signal of the second band will behave like noise. The use of band-splitting receivers on ground-based telescopes is attributable to a gain in the signal-to-noise ratio compared to two-band receivers because of a twofold reduction of the contribution of thermal noise from the atmosphere and the receiver's optics to the overall noise temperature of the system by eliminating the contribution of mirror-band noise. It should be noted that this gain occurs in the case of observing spectral lines and ther is no such gain in the study of broadband signals present simultaneously in both bands of a local oscillator receiver. Currently, a search is actively underway for promising sites for the creation of a submillimeter telescope in the Russian Federation [9–11]. We have to consider sites where the integral water content in the atmosphere is of the order of 2−4 mm in the realistic case due to the absence of high-altitude desert areas in our country comparable to the Chajnantor plateau, where the ALMA [2] and APEX [4] telescopes are located at an altitude of more than 5000 m above sea level. The atmospheric transparency in the range of 1.1−1.4 mm will average about 0.8 under these conditions [12,13]. The noise contribution of the atmosphere in each band can be estimated at approximately 50 K in this case, which is comparable to the expected noise temperature of the mixer, and gives a strong motivation for using a receiver with band separation.

A recent simulation of the complete waveguide structure of a sideband-separated mixing system has shown that the level of reflection from embedded waveguide loads should not exceed −20 dB at an operating temperature of 4 K [14]. Otherwise, achieving the desired quality of sideband separation in −15 dB will be a difficult task. In this case, it is preferable that the reflection from the waveguide load is reduced to −30 dB. In this case, the task of designing and manufacturing the entire waveguide structure for a receiver with high-quality band separation will be significantly simplified by reducing the requirements for the accuracy of waveguide structures, as well as for their size limits. These arguments provide an incentive for

developing the cryogenic waveguide load described in this paper.

There are a number of solutions for creating waveguide loads operating in the millimeter and submillimeter wavelength range at cryogenic temperatures. Most of these solutions use dielectric absorbers of various shapes. Absorbers can either be installed in the waveguide [5,15,16], or placed in a special cavity at the end of the waveguide [17]. However, the fundamental feature of these loads is that they are made from a specific dielectric material MF-112 and MF-116 [16], which is produced only in the USA. This limitation was one of the main reasons for making the decision to develop the load independently. A common industrial method for creating waveguide loads up to 50 GHz is the use of ferrite powder mixed with epoxy resin. Creating a load of this type for cryogenic temperatures and for frequencies above 200 GHz will require a dedicated technological R&D. At the same time, the use of the above waveguide inserts poses difficulties for assembling the entire waveguide block with band separation, since this block will require the use of at least three such loads [14]. Inserts should be placed in one half of the block and will extend beyond the docking area, and the second half should be put on them. To do this, the inserts should be made in a reduced size, which carries a risk for their absorbing properties. We chose a load option based on a knife insert to avoid this difficulty, which can be completely placed inside one of the halves of the waveguide block and will not mechanically affect the alignment with the other half.

1. Waveguide load design

One of the classic solutions for creating waveguide loads and tunable attenuators is to use a knife insert (see, for example, [18]). A similar solution was chosen for our development presented in this paper (Fig. 1). The load is a plate of amorphous quartz with a thickness of 125 μm. A film of resistive material is applied to one of the sides of the plate. The shape of the plate is a rectangle of size 5×1.5 mm with two truncated corners. The non-truncated wide side of the rectangle is the base of the plate with a length of 5 mm, and the side parallel to it is the narrowed vertex of the load, which has a width of 1 mm. The flat vertex should fit closely to the far wall of the waveguide, so that the entire inclined part formed as a result of truncating the corners of the rectangle passes from one to the other side of the waveguide in the plane along the electric field vector of the first waveguide mode.

The dimensions of the waveguide into which the load is to be inserted are $1000 \times 500\,\mu$m. These values are determined by the previously developed single-band SIS mixer [19] and the waveguide block designed for it [14,20]. The load is placed in a special cavity with a depth of 140 μm in one of the halves of the split unit, which guarantees high-quality and reliable installation. The surface of the plate on which the metal is applied is almost exactly in the middle of the waveguide.

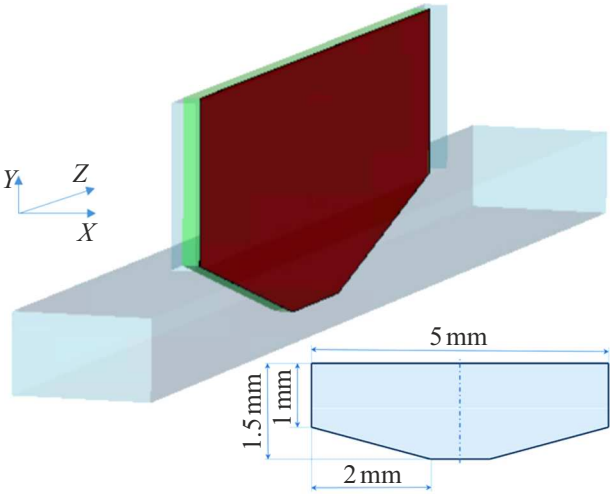

Figure 1. 3*D*-type of waveguide load inserted in the waveguide. The lower part of the figure shows the dimensions of the designed load.

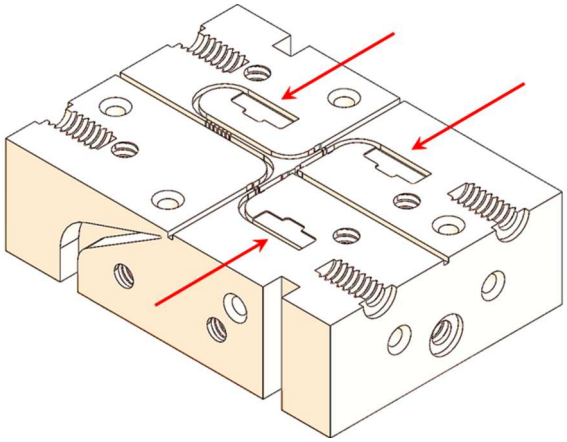

Figure 2. Half of the waveguide block of the SIS-mixer with separation of side bands, constructed taking into account the designed waveguide load.

Three identical loads will be installed in the waveguide unit of the SIS-mixer with separate side strips, so they are compact enough to fit in it, but at the same time have sufficiently large dimensions that are convenient for reliable placement and installation. Figure 2 shows the appearance of the half of the waveguide unit in which the three loads will be mounted. They will be placed in the cavities shown by the arrows. Two of them are used to absorb unused power from the reference generator, and one is used to absorb reflections from the SIS-mixers and the quadrature divider. A detailed description of the elements of the presented waveguide block and their functionality can be found in the articles in Ref. [14,20]. Figure 3 shows the dimensions of the mounting cavity, which exceed the

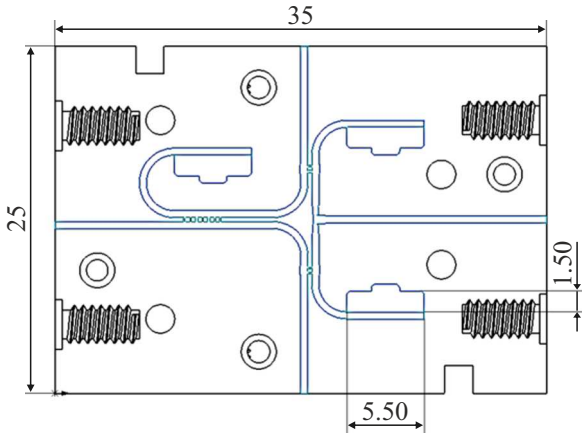

Figure 3. Dimensional drawing of half of the waveguide block.

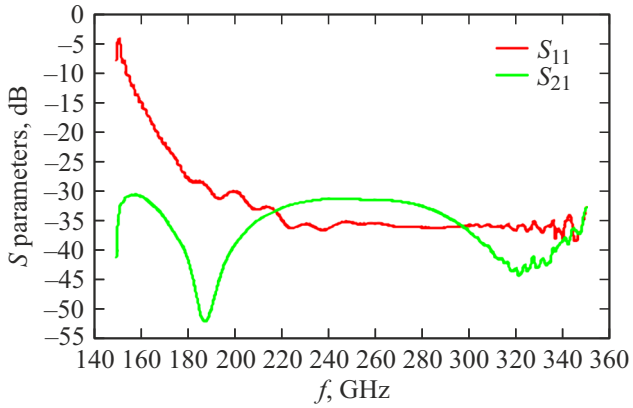

Figure 4. Calculated values of reflection S_{11} and transmission S_{21} for the designed waveguide load.

dimensions of the load itself, which will allow convenient placement and precise installation of it. Any adhesive can be used for securing the insert in the cavity, which does not necessarily have a high conductivity, since the conductive surface of the load is shorted to the walls of the waveguide at a high frequency due to capacitive coupling. At the same time, it should be taken into account that the adhesive should guarantee high-quality heat removal, since the power of the absorbed signal from the reference generator is significant and can cause additional heating.

2. Modeling of frequency characteristics

The results of modeling of frequency characteristics are shown in Fig. 4. The calculations were performed using a three-dimensional electromagnetic simulator. Calculations are performed for the nominal design resistance of a metal film of 250 Ω/sq. The material of the waveguide walls and surroundings is taken as an ideal conductor, which is justified due to the extremely small losses in the existing short waveguide. Taking into account resistive losses in the waveguide walls can only improve the absorbing characteristics of the load. Figure 4 shows that the reflection level of S_{11} does not exceed −35 dB for frequencies above 220 GHz. The graph also shows the transmission curve S_{21}, which has a level of no more than −30 dB. This level guarantees high-quality absorption of the microwave signal in the load and allows you to neglect in the future the fraction of radiation that passes through the load. This is explained by the fact that the signal reflected behind the load undergoes repeated passage through it and its relative value weakens already below the level of −60 dB, and cannot significantly affect the overall picture for S_{11}.

The effect of the accuracy of installation of the load in the waveguide on the final microwave parameters was analyzed for assessment of the risk associated with possible errors in the shape of the load or waveguide, or with errors in the position of the load relative to the waveguide during installation. Fig. 5, *a, b* shows changes in the reflection level

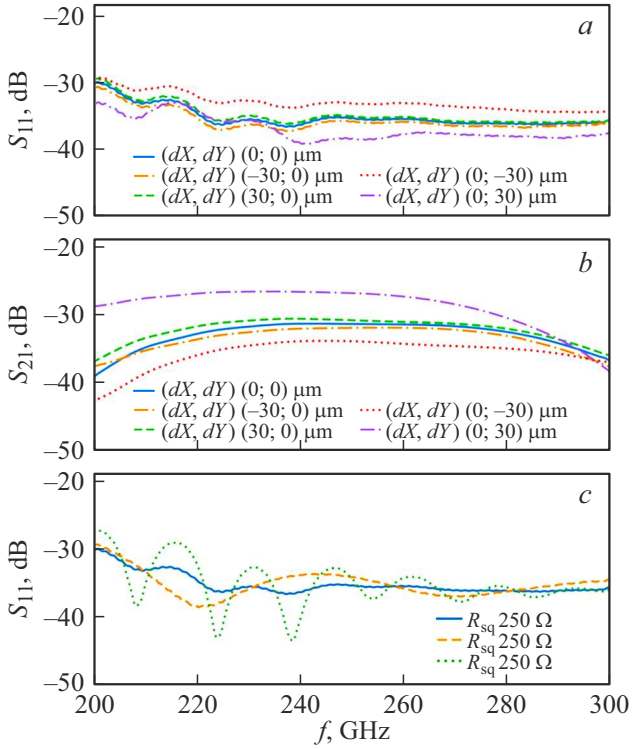

Figure 5. *a* — dependence of the reflection level on the load S_{11} on the frequency with the varying position of the load; *b* — dependence of the transmission level of the load S_{21} on the frequency with the varying position of the load (the offset directions are shown by the corresponding axes in Fig. 1); *c* — dependence of the reflection level on the load S_{11} on the frequency with the varying resistance of the metal film.

and transmission level in case of inaccuracies in extending the load into the waveguide (dY), as well as in case of errors in the load position relative to the dividing plane of the split block (dX), which may be caused by inaccuracy in the manufacture of the load-bearing recess, as well as by debris falling under it during installation. It can be seen from the above dependence that the reflection level remains

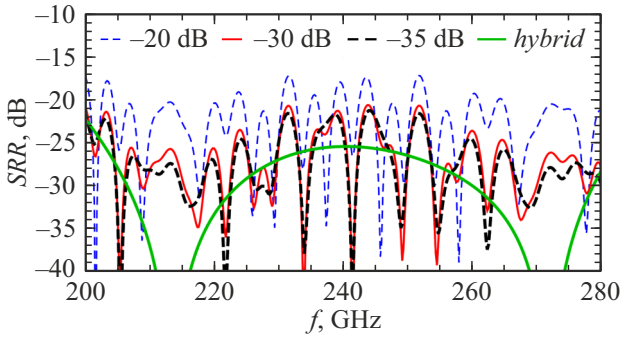

Figure 6. Calculated frequency dependence of band separation quality *SRR* for various load reflection levels ranging from −20 to −35 dB. The „hybrid“ curve is shown for comparison that looks as *SRR* in the case of complete absence of reflections in the waveguide block.

obviously lower than −30 dB for significant deviations up to 30 μm that can be reliably detected by a measuring microscope, which makes the practical implementation of such a load realistic. It is interesting to note that pushing the load into the waveguide not completely ($dY = 30\,\mu$m) provides an even greater reduction of the reflection level S_{11}. At the same time, S_{21} begins to increase slightly above −30 dB. This is still not critical at all, but it clearly indicates an increasing negative impact when deviations greater than the presented 30 μm, and warns against further deliberate shifting of the load in this direction. The presented deviations dX and dY clearly correspond to the axes indicated in the general load view in Figure 1.

In addition to the deviation in the load position, a variation in the parameters of the absorbing metal film, in particular, its resistance, is very likely. Such a deviation can occur due to differences in the conductivity of the thin metal film sprayed on quartz from the nominal 250 Ω both due to manufacturing conditions, and due to temperature changes during cooling to 4 K. Modeling of the reflection level for different film resistances is illustrated in Fig. 5, *c*. Even with a significant change of resistance from 100 to 400 Ω/sq, the reflection level remains below −30 dB, which shows an extremely weak dependence of the load quality on the resistance of the metal film. The demonstrated extreme resistance of the load design to variations in film resistance indicates its high degree of practicality and reliability. The resulting periodic pattern for the reflection curves S_{11} at a resistance per square of 400 Ω is attributable to the superposition of several weak reflections, which begin to appear due to less absorption in the load itself.

To evaluate the effect of the load reflection level on the overall Sideband Rejection Ratio, *SRR* for the already designed waveguide block structure presented in Ref. [20], additional simulations of the entire receiver waveguide structure are performed, taking into account the reflections described in detail in Ref. [14]. The SRR level dependencies are obtained for three cases: −20, −30, −35 dB. A comparison of these curves is shown in Fig. 6. Calculations are made for the level of reflection from the SIS-mixers −3.3 dB. It can be seen that the improvement of load reflections from −20 to −30 dB can result in a decrease of SRR at the worst points from approximately −17 to −21 dB, which is a significant change. Further reduction of reflections to −35 dB results in small changes of the quality of band separation, approximately by 1 dB. This is attributable to the fact that the contribution of reflections involving SIS-mixers and the load becomes much smaller than the signal distortions that occur due to reflections from SIS-mixers that leak through the insulation of the quadrature bridge and do not interact with the waveguide load in any way. These types of reflections are described in detail in Ref. [14]. For comparison, Figure 6 shows the „hybrid“ curve, which shows the level of band separation quality that would occur if there were only distortion introduced by a quadrature bridge, also called a hybrid splitter. This quality of band separation would be achieved if there were no reflections or imbalances in the rest of the receiver.

It should be noted that the presented estimate calculations are made for a relatively simplified case, namely, when the possible difference of the gain of two single SIS-mixers used in a band-separated receiver is not taken into account, and the phase distortion between the reference generator signals coming to single SIS-mixers, which also occurs because of reflections of signals from SIS-mixers and waveguide loads. Taking these factors into account will make an even greater difference in the SRR change when the reflection level varies from the developed waveguide load.

3. Fabrication of the metal film

A Ti layer with a thickness of less than 10 nm was used as a load resistive material in the article in Ref. [18], which was then actively oxidized on the surface to protect the titanium film itself from subsequent degradation in the atmosphere. Also, the final thickness of the film was selected to achieve the required level of resistance by the controlled oxidation of a part of the film. The aim of this work was to obtain a heated load for calibration of waveguide devices due to a local change in the load temperature. However, Ti can significantly change the resistance between room and cryogenic conditions. We decided to use a thin NiCr film for this reason. It is fundamentally important that the resistance of such films should vary very slightly with temperature, even when cooled to 4 K. This will significantly simplify the process of testing such loads, as it will allow measuring the reflection coefficient at room temperature with confidence that similar characteristics will also be manifested in the cryogenic conditions [21].

As a result, in the framework of this work, the film deposition by magnetron sputtering using a NiCr target with a ratio of the proportion of the corresponding metals 60/40 was worked out. Sputtering was performed in an argon atmosphere at a pressure of $7 \cdot 10^{-3}$ mbar. NiCr film with a thickness of about 8 nm is formed on the quartz substrate

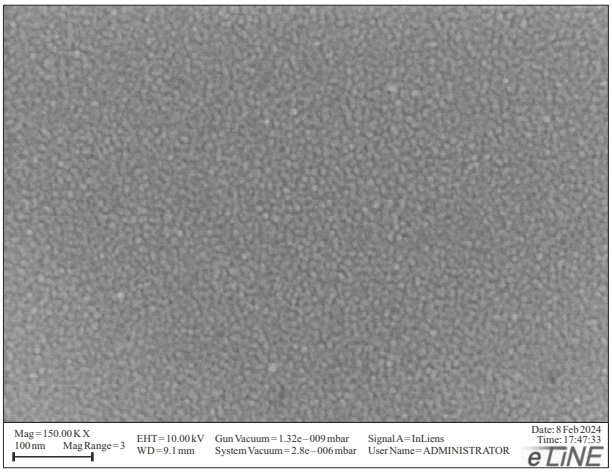

Figure 7. The result of an electron microscope scanning of the surface of a deposited NiCr film having a thickness of 8 nm. The size label is shown in the lower-left corner.

during the sputtering time of 12 s. As shown by direct current measurements performed at different temperatures, the resistance of the resulting film is 251 Ω/sq at 300 K, 253 Ω/sq at 77 K and 257 Ω/sq at 4.2 k. Thus, the variation of the resistance from room to cryogenic conditions was less than three percent, which, taking into account the nature of the curves shown in Fig. 5, allows expecting negligibly small changes of the reflection level during cooling.

The surface of the film was scanned using an electron microscope to verify the uniformity of the resulting NiCr films. The result of the resulting image is shown in Fig. 7. It can be seen that the film grows evenly, breaks are almost completely absent, and the characteristic size of granules that almost inevitably occur during spraying is less than 10 nm, which is comparable to the thickness of the film itself. This allows making conclusion that the film is applied continuously and will definitely work as a homogeneous material for microwave signals in the operating frequency range, i.e. above 200 GHz. All this makes it possible to count with high probability on a good agreement between the calculated and future experimental parameters of the entire waveguide load.

Conclusion

A cryogenic waveguide load is designed for the range 1.1−1.4 mm, made in the form of a knife insert in the center of the waveguide, which is an amorphous quartz substrate with a thickness of 125 μm with a thin NiCr alloy film deposited on it with a thickness of about 8 nm. The resistance of the fabricated metal film is about 250 Ω/sq and changes by less than 3 when cooled to cryogenic temperatures (4 K), which allows fully characterizing the load in room conditions and provides confidence with a high degree of probability in its equally high-quality operation and in cryogenic conditions. Calculations show that the level of reflections from the load should not exceed −35 dB in the range of 220−330 GHz, which meets the requirements for a receiver with sideband separation with a margin. At the same time, modeling of the load operation with realistic manufacturing and installation error parameters of 10 μm shows that the reflection level is guaranteed to remain within the value −30 dB in the required frequency range. At the next stage of work we plan to directly fabricate the loads and conduct a study of their properties in a special test unit at room temperature and under cryogenic conditions. Next, the loads will be installed in the already developed waveguide unit and tested as part of a full-fledged IC receiver with a separation of the side bands of the range 1.1−1.4 mm.

Acknowledgements

We express our sincere gratitude to our colleagues M.A. Tarasov and M. Strelkov for fruitful conversations and proposed ideas, which fundamentally affected the success of the work carried out. The equipment of UNU #352529 „Kriointegral“ was used for fabrication and studying the samples.

Funding

Load design and calculation of its VHF properties were carried out at the expense of the Russian Science Foundation grant (№ 23-79-00061, https://rscf.ru/project/23-79-00061/). The work for debugging the load fabrication technology is supported by the Ministry of Science and Higher Education of the Russian Federation (Agreement № 075-15-2024-538).

Conflict of interest

The authors declare that they have no conflict of interest

References

[1] A. Wootten, A.R. Thompson. Proc. IEEE, **97** (8), 1463 (2009).
[2] *ALMA Observatory Website*. Available online: https://www.almaobservatory.org/en/about-alma/
[3] A.M. Baryshev, R. Hesper, F.P. Mena, T.M. Klapwijk, T.A. van Kempen, M.R. Hogerheijde, B.D. Jackson, J. Adema, G.J. Gerlofsma, M.E. Bekema, J. Barkhof, L.H.R. de Haan-Stijkel, M. van den Bemt, A. Koops, K. Keizer, C. Pieters, J. Koops van het Jagt, H.H.A. Schaeffer, T. Zijlstra, M. Kroug, C.F.J. Lodewijk, K. Wielinga, W. Boland, M.W.M. de Graauw, E.F. van Dishoeck, H. Jager, W. Wild. A&A, **577**, A129, (2015). https://doi.org/10.1051/0004-6361/201425529
[4] R. Güsten, R.S. Booth, C. Cesarsky, K.M. Menten, C. Agurto, et. Al. Proc. SPIE, **6267**, 626714 (2006).
[5] D. Maier, J. Reverdy, D. Billon-Pierron, A. Barbier. SSB, **4** (8), 129 (2014).
[6] P.T. Ho, J.M. Moran, K.Y. Lo. Astrophys. J., **616** (1), L1-L6 (2004).

[7] I.D. Novikov, S.F. Likhachev, Yu.A. Shchekinov, A.S. Andrianov, A.M. Baryshev, A.I. Vasyunin, D.Z. Wiebe, Th. de Graauw, A.G. Doroshkevich, I.I. Zinchenko, N.S. Kardashev, V.I. Kostenko, T.I. Larchenkova, L.N. Likhacheva, A.O. Lyakhovets, D.I. Novikov, S.V. Pilipenko, A.F. Punanova, A.G. Rudnitsky, A.V. Smirnov, V.I. Shematovich. Phys.-Uspekhi, **64** (4), 386 (2021). https://doi.org/10.3367/ufne.2020.12.038898
[8] *Millimetron Space Observatory Website*. Available online: http://millimetron.ru/index.php/en/
[9] I.I. Zinchenko A.V. Lapinov, A.V. Lapinov, V.F. Vdovin, P.M. Zemlyanukha, T.A. Khabarova. Appl. Sci., **13** (21), 11706 (2023). https://doi.org/10.3390/app132111706
[10] V.B. Khaikin, A.Y. Shikhovtsev, A.P. Mironov, X.A. Qian. *A Study of the Astroclimate in the Dagestan Mountains Agul Regionand at the Ali Observatory in Tibet as Possible Locations for the Eurasian SubMM Telescopes (ESMT)* In Proceed. of the The Multifaceted Universe: Theory and Observations — 2022 (Nizhny Arkhyz, Russia, 2022), p. 72.
[11] A.Y. Shikhovtsev, V.B. Khaikin, A.P. Mironov, G.P. Kovadlo. Atmos Ocean Opt., **35**, 168 (2022).
[12] A. Otarola, M. Holdaway, L.E. Nyman, S.J.E. Radford, B.J. Butler. *Atmospheric Transparency at Chajnantor*: 1973−2003, in ALMA Memo Series, 2005, Memo 512. [Online]. Available: http://library.nrao.edu/ alma.shtml
[13] Electronic source. Available at: http://www.apex-telescope.org/weather/.
[14] A. Khudchenko, I. Tretyakov, V.P. Koshelets, R. Hesper, A.M. Baryshev. IEEE Transactions on Terahertz Sci. Technol., **13** (6), 645 (2023).
[15] A.R. Kerr et all. Proc. IEEE MTT-S Int. Microw. Symp. Dig., 1 (2013).
[16] A.R. Kerr, H. Moseley, E. Wollack, W. Grammer, G. Reiland, R. Henry, K.P. Stewart. NRAO, ALMA Memo, 14 May 2004.
[17] R. Hesper, A. Khudchenko, A.M. Baryshev, J. Barkhof, F.P. Mena. Millimeter, Submillimeter, and Far-Infrared Detectors and Instrumentation for Astronomy VIII. **9914**, 79 (2016).
[18] J.W. Kooi et al. IEEE Transactions on Terahertz Sci. Technol., **8** (4), 434 (2018).
[19] K.I. Rudakov, A.V. Khudchenko, L.V. Filippenko, M.E. Paramonov, R. Hesper, D.A.R., da Costa Lima, A.M. Baryshev, V.P. Koshelets. Appl. Sci., **11** (21), 10087 (2021).
[20] I.V. Tretyakov, A.V. Khudchenko, R.A. Cherniia, S.F. Likhachev. J. Commun. Technol. Electron., **68** (9), 989 (2023).
[21] M.V. Strelkov, A.M. Chekushkin, A.A. Gunbina, M.A. Tarasov. IEEE 8th All-Russian Microwave Conference (RMC), 49 (2022).

Translated by A.Akhtyamov